Reference to be cited:

Romanazzi, A., Gentile, F., Polemio, M.: Modelling and management of a Mediterranean karstic coastal aquifer under the effects of seawater intrusion and climate change, Environmental Earth Sciences, 74 (1), 115-128, DOI: 10.1007/s12665-015-4423-6, 2015.

INDEX

Reference to be cited:
Romanazzi, A., Gentile, F., Polemio, M.: Modelling and management of a Mediterranean karstic coastal aquifer under the effects of seawater intrusion and climate change, Environmental Earth Sciences, 74 (1), 115-128, DOI: 10.1007/s12665-015-4423-6, 2015.

Modelling and management of a Mediterranean karstic coastal aquifer under the effects of seawater intrusion and climate change

Romanazzi A.[1], Gentile F.[2], Polemio M.[1]
1 – CNR IRPI – Bari, via Amendola, 122/I
2 – University of Bari – Department DISAAT - via Amendola, 165/A
Corresponding Author: m.polemio@ba.irpi.cnr.it

Abstract: The study and management of the groundwater resources of a large, deep, coastal, karstic aquifer represent a very complex hydrogeological problem. Here, this problem is successfully approached by using an equivalent porous continuous medium (EPCM) to represent a karstic Apulian aquifer (southern Italy). This aquifer, which is located on a peninsula and extends to hundreds of meters depth, is the sole local source of high-quality water resources. These resources are at risk due to overexploitation, climate change and seawater intrusion.

The model was based on MODFLOW and SEAWAT codes. Piezometric and salinity variations from 1930 to 2060 were simulated under three past scenarios (up to 1999) and three future scenarios that consider climate change, different types of discharge, and changes in sea level and salinity. The model was validated using surveyed piezometric and salinity data.

An evident piezometric drop was confirmed for the past; a similar dramatic drop appears to be likely in the future. The lateral intrusion and upconing effects of seawater intrusion were non-negligible in the past and will be considerable in the future. All phenomena considered here, including sea level and sea salinity, showed non-negligible effects on coastal groundwater.

Keywords: karstic coastal aquifer, numerical modelling, seawater intrusion, climate change.

1. Introduction

Water is the most important resource for the survival of living organisms, including human health and related activities. Fresh water is distributed globally as follows: approximately 69.7% exists in the form of perennial ice, 30% in groundwater resources and only 0.3% in the form of surface water (Oude Essink 2001).

Groundwater annually supports $230 billion of agricultural production and supplies freshwater for one-third of the world’s population (Oude Essink 2001). In addition, groundwater is essential for the development of groundwater-dependent ecosystems.

Groundwater discharge increased over the second half of the 20th century, and a great number of aquifers worldwide are now overexploited. This overuse is concentrated in coastal areas, where increasing population, growth of urban areas, and increasing irrigation, industrial, and tourism needs are occurring (Pisinaras et al. 2007; Ersoy and Gultekin 2008; Polemio et al. 2008; Shammas and Thunvik 2009; Garcia-Ruiz et al. 2011; Polemio et al. 2011).

Karstic aquifers supply 7-10% of the groundwater resources used worldwide and 29% of those in Europe. The majority of these aquifers are coastal aquifers (Biondic and Bakalowicz 1975; COST 2005).

Karst waters are the only water resources in many countries, but due to particular characteristics such as thin soils, point recharge in dolines and swallow holes and high hydraulic conductivity, karstic aquifers and environments are highly vulnerable to contamination and to anthropogenic modifications. The residence time of groundwater in these aquifers is generally short, and consequently, contamination propagates and occurs much more quickly than in non-karstic aquifers. Any modifications to the quality and availability of current coastal karstic groundwater outflow can severely affect the hydrological and ecological equilibriums of the sea and of coastal wetlands. In addition to anthropic pollution, karstic coastal aquifers are vulnerable to seawater intrusion.

The primary effects of aquifer overexploitation, i.e., declining piezometric levels, are amplified in coastal aquifers in terms of quality degradation due to seawater intrusion.

Most of the coastal aquifers of Mediterranean countries, such as Spain, France, Portugal, Slovenia, Croatia, Greece, Albania, Turkey, Morocco, Palestine and Italy, are karstic and are at risk of overexploitation and seawater intrusion (Fig. 1) (Biondic and Bakalowicz 1975; EEA 1999; Lambrakis and Kallergis 2001; Qahman and Larabi 2004; Polemio et al. 2005; Gomez et al. 2003;Barrocu 2003; COST 2005; Polemio 2005; Davraz et al. 2009; Custodio 2010; Baalousha 2011; Mutasem et al. 2014).

At same time, many signs indicate that the climate of the Mediterranean basin, a traditional transition zone between the arid North African and the temperate European climate, may be changing so much as to suggest a transition towards a tropical climate (IPCC 2007). This climate change, particularly with regard to changes in temperature, precipitation, sea level, and sea water salinity, should be a key factor affecting the longevity of groundwater resources of coastal Mediterranean aquifers (IPCC, 2007). Moreover, an indirect but relevant effect of climate change and droughts in the Mediterranean is the increase in the trend towards overexploitation and the consequent exacerbation of seawater intrusion (Cotecchia et al 2003; Cost 2005; Polemio 2005; Giorgi and Lionello 2008; Candela et al. 2009; Garcia-Ruiz et al. 2011). The combined effects of decreasing recharge and increasing discharge are likely to drastically affect the availability and quality of coastal groundwater resources. These trends have also been observed in Italy, where seawater intrusion is the main cause of groundwater quality degradation in coastal karst aquifers.

For these reasons, it is critical to develop management tools for the sustainable use of groundwater resources of karstic coastal aquifers. Numerous studies concerning numerical modelling of coastal karst aquifers have been conducted on local scales (Lambrakis and Kallergis 2001; Qahman and Larabi 2006; Pisinaras et al. 2007; Giambastiani et al. 2007; Rejani et al. 2008, Shammas and Thunvik 2009; Candela et al. 2009; El-Bihery 2009; Cobaner et al. 2012; El Ayni et al. 2013). Large-scale analyses have often been based on simplified GIS approaches, whereas reliable numerical modelling is relatively rare, especially for management purposes (Sutanudjaja et al. 2001; Langevin 2003; Masciopinto 2006; Ranjan et al. 2006).

A regional (at the hydrogeological basin scale) approach that considers seawater intrusion, climate change, sea level and sea salinity changes together with anthropogenic perturbations is proposed to analyse a wide karstic coastal aquifer. The core of the approach is a large-scale numerical model based on an equivalent porous continuous medium (EPCM). The approach is applied to the case of Salento (Apulia region, southern Italy), a peninsula that hosts a large, deep karstic hydrogeological basin that is used to discharge high-quality groundwater for all uses due to the lack of local superficial water resources. The modelling was specified to simulate groundwater quality and quantity modifications beginning in the 1930s and extending to different future scenarios that reflect the combined effects of natural and anthropogenic modifications of groundwater resources.

2. Hydrogeological regional characteristics and the selected hydrogeological basin

The coastline of the Apulia region is 800 km in length. The region hosts the largest coastal karstic Italian aquifers. Large limestone and dolomite Mesozoic outcroppings constitute the physiographic units of Gargano, Murgia and Salento; outcroppings of detrital organogenic soils and rocks (Tertiary and Quaternary) can be found in the topographic troughs that partially overlap the above-mentioned carbonate rocks (Fig. 2) (Maggiore and Pagliarulo

2004, Cotecchia et al. 2005). Four hydrogeological structures (HSs) can be distinguished in the Apulian region: Tavoliere, Gargano, Murgia and Salento, the last three of which are karstic.

The Tavoliere HS is characterised by a porous shallow aquifer whose groundwater flow is limited by a clay bottom a few hundred meters thick. The Tavoliere HS hosts aquifers of secondary relevance, whereas the karstic HSs (Mesozoic rocks) create large carbonate aquifers that are hundreds of meters deep and are deeply influenced by karstic phenomena. These aquifers exhibit varying degrees of fracturing and permeability (Polemio et al. 2009a).

Gargano is a high horst that strikes NE-SW in the shape of a promontory extending into the Adriatic Sea. The carbonate rock types of Gargano allow it to be divided into two distinct parts: the eastern sector is made up of frontal reef depositions and transition depositions, and the central-western sector is dominated by reef facies rocks and, to a lesser degree, by back reef depositions. Due to the mountainous features of Gargano, the level of anthropogenic activities is very low as the level of groundwater utilisation (Polemio et al. 2000; Cotecchia et al. 2005).

Murgia HS, which corresponds to a plateau (peak altitude 680 m asl) and has a large asymmetric horst caged in by two direct fault systems (striking NW-SE and NE-SW), and Salento HS, an almost flat area (peak altitude 150-180 m asl) bounded by two seas, together constitute a continuum for groundwater flow. These HSs are also divided by a morphological-structural feature called the Messapian Threshold, which is multiple kilometres wide and covers an area that extends from sea to sea (Fig. 1 and Fig. 3) (Cotecchia et al. 2005). Moving from Murgia to Salento HS, the hydrogeological parameters improve (in the latter, higher hydraulic conductivity and storage coefficients are observed), the depth to water decreases considerably (from hundreds to tens of meters), the mean piezometric head decreases, the mean distance from the sea decreases, the level of groundwater utilisation increases, and, on the whole, the risk of quality degradation as a result of seawater intrusion increases (Cotecchia and Tulipano 1989; Polemio 2005).

Recharge of both these HSs occurs mainly from rainfall infiltration, but a large amount of the Murgia recharge discharges to the sea by flowing across the Salento HS. Focusing on groundwater flow and the piezometric surface, a hydrogeological boundary divides the Salento HS into two portions: the northern portion, in which the main inflow is due to recharge from the Murgia HS and discharge is to the Ionian and Adriatic Seas, together with direct rainfall infiltration, and the southern portion, in which the recharge is only due to direct rainfall infiltration. This southern portion of the Salento area experiences greater effects of seawater intrusion (Polemio et al. 2008).

The study area focuses on the southern portion of the Salento HS. The hydrogeological boundary of no flow between northern and southern Salento portions was identified from piezometric data from the 1930s, the decade in which groundwater discharge by wells was beginning but was still very low or negligible (Fig. 3), and validated with piezometric maps from the 1970s, 1990s, 2003, and 2007 (Polemio et al. 2011). The hydrological basin thus defined is the study area and is approximately 2,400 km^2 wide.

All types of relevant geological, geomorphological and hydrogeological features were implemented in a geodatabase and analysed in a GIS environment using a DEM (digital elevation model) as the reference ground surface. Starting with 25×25 m resolution, the DEM was integrated with bathymetric data to obtain a continuous surface with a 75×75 m resolution, merging ground topography and bathymetry. A special effort was undertaken to focus on any information useful to characterising the karstic features affecting groundwater flow (Fig. 4). The study area is mainly bounded by the coastline, which is 175 km in length.

Five hydrogeological complexes can be distinguished: limestone, calcarenite-calcilutite, calcarenite, clay, and sand-conglomerate-calcarenite (Fig. 4). A schematic description of these complexes and of their geometrical features and relationships is provided (Fig. 5) (Cotecchia 1977, Ciaranfi et al. 1988, Cotecchia et al. 2005).

The limestone complex, which includes carbonate rocks of some geological formations, mainly the Altamura Limestone and secondly the Castro Limestone and Porto Badisco Calcarenites, shows permeability ranging from medium to very high due to karstic and fracturing processes, resulting in the most permeable complex in the studied area. This complex outcrops inland while moving towards the coastline, especially eastward; in areas without outcrops, the complex is overlain by the one of the other complexes (Fig. 5). The bottom of the limestone complex, which is not intercepted by the studied wells, must therefore be located at deep depths (thousands of meters). These depths are indefinable and thus not relevant for hydrogeological purposes. Moreover, this complex corresponds locally to the deep Apulian limestone aquifer, which involves Murgia and Salento HSs (Fig. 1).

The calcarenite-calcilutite hydrogeological complex, which is mainly associated with the geological formations of Pietra Leccese and Andrano Calcarenites, is characterised by permeability from medium-low to medium and a general thickness of 50 to 150 m. The limestone complex is at the bottom; the calcarenite complex is at the top, where it does not outcrop.

The calcarenite hydrogeological complex, which is mainly associated with the geological formations of Gravina Calcarenite, exhibits medium permeability and a general thickness of 50 to 100 m. The clay or sand-conglomerate-calcarenite complex is at the top, where it does not outcrop.

The combined hydrogeological effect of the calcarenite-calcilutite complex and the calcarenite complex is to create a lower-permeability cover for the main aquifer. This effect is minimal and almost negligible at the regional scale for the effect of local vertical discontinuities caused by fracturing and karstic features (Tulipano and Fidelibus, 1988).

The clay hydrogeological complex, which is mainly associated with the geological formations of sub-Apennine clays, shows very low permeability. This complex does not outcrop, and it forms the bottom of the sand-conglomerate-calcarenite complex.

The sand-conglomerate-calcarenite hydrogeological complex, which mainly contains marine terraced deposits, exhibits medium permeability, with areas of medium-high permeability. The average complex thickness is low; the peak value is approximately 50 m. This condition creates a shallow aquifer underlain by the clay complex.

Two types of aquifers can be distinguished: the deep or karstic aquifer, which is continuous over broad areas, and narrow, shallow, and discontinuous aquifers. Shallow aquifers, due to their low thickness and relatively low permeability, are of secondary importance and will not be discussed in detail.

In the selected hydrogeological basin, the karstic aquifer is exclusively fed by rainwater falling in the study area. Natural discharge or aquifer outflow results from a number of diffuse and concentrated coastal springs, the majority of which are submarine (Cotecchia and Tulipano, 1989). The hydrogeological conceptual model was developed on the basis of these conditions and features (Fig. 5).

The coastal karstic aquifer can be considered a classic case of seawater intrusion in a permeable peninsula: a fresh groundwater lens that floats on saline water due to seawater intrusion (Cotecchia 1977, Maggiore and Pagliarulo 2004). In this context, seawater intrusion is a pervasive phenomenon that afflicts fresh groundwater resources (Cotecchia 1977; Polemio 2005).

A declining trend in the spatial mean of piezometric surfaces has been observed since the 1970s (Polemio et al. 2009b, 2011). A 500 mg/L salinity threshold between pure, fresh groundwater and groundwater mixed with saline water due to seawater intrusion was defined in the case of Apulian coastal karstic aquifers; a withdrawal trend of a 500 mg/L salinity contour line was observed as an effect of recent (since the 1970s) periods of severe drought (Polemio et al. 2009a) and as an effect of lateral seawater intrusion. An increasing trend in salinity was observed in each considered well with data from 1969 to 2001. Chloride concentration trends from 0.06 to 5.72 mg/(L yr) were measured in these wells (Polemio and Limoni 2001, Polemio et al. 2008). Upconing effects due the long-standing discharge for drinking water were detected in the central portion of the hydrological basin (Cotecchia et al. 2002).

2.1 Hydrological balance and recharge assessment

Monthly temperature and rainfall data from 15 gauges located inside or close to the study area were collected from 1930 to 1999. The main purpose was to define the recharge in natural and steady conditions. The period 1930-1979 (50 years) was selected as a reference period over which to assess the mean natural recharge rates considering the following circumstances: 1) the level of groundwater well discharge was low and negligible in the 1930s and has generally increased since the 1970s due to an increasing number of bored wells (Polemio et al. 2010); 2) the effects of climate change were low or negligible from the 1930s to the 1970s in the whole of southern Italy (Polemio and Casarano 2004).

In the Mediterranean basin, there is a linear correlation between altitude and rainfall or temperature; a secondary but non-negligible influence of the distance from the sea is also a factor (Polemio et al. 2000, Civita 2005). On this basis, multiple linear regression functions of mean annual rainfall, R, and temperature, T, were defined as a function of altitude, Z (m asl), and distance, D (km), from the Adriatic coast:

$$P = 673.73+1.585z-3.414D \quad (R^2 = 0.84) \qquad (1)$$

$$T = 16.91-0.00809z +0.015D, (R^2 = 0.93) \qquad (2)$$

Using a GIS environment, P and T were assessed for each DEM cell. The spatial mean of P in the hydrological basin was 730 mm. T ranged from 16.0 to 17.5 °C in the study area. The mean annual actual evapotranspiration, calculated using the modified Turc method (Polemio et al. 2000), ranged between 473 and 602 mm, with 553 mm as the spatial mean. The actual rainfall was calculated cell by cell as the difference between the rainfall and effective evapotranspiration.

The infiltration was calculated cell by cell by multiplying the infiltration coefficient by the net rainfall. The infiltration coefficient, i.e., the ratio of the mean annual infiltration to the mean annual net rainfall, was assessed based on previous data on the hydrological balance of aquifers under similar climatic and hydrogeological conditions (Polemio et al. 2000, Civita 2005). The values used are 0.90, 0.60, 0.65, and 0.70 for limestone, calcarenite-calcilutite, calcarenite, and sand-conglomerate-calcarenite complexes, respectively (the clay complex does not outcrop). The infiltration coefficient was considered equal to 1 in each cell corresponding to an endorheic area for any outcropping hydrogeological complex. The results were used to define recharge rates in steady-state conditions and to simulate the first past scenario, P1, from 1930 to 1979.

These calculations were repeated for two additional past scenarios P2 (1980-1989) and P3 (1990-1999) using monthly rainfall and temperature data from each period. P2 included a severe and long-lasting drought.

3. Numerical modelling

Coastal karstic aquifers can be considered anisotropic and inhomogeneous at the local scale due to fractures and karstic features. Discrete fracture network or dual porosity modelling approaches can be used in these cases (USA NRC 1996). These approaches, however, require a large amount of information on the geometrical parameters of fractures that may be very difficult to obtain on the appropriate local scales.

However, if the rock system shows a high density of interconnected fractures and voids, it can be considered to behave as an EPCM, particularly if the modelling is performed on a regional scale (Andreson and Woessner 1992; Huntoon 1994; Dufrense and Drake 1999; Abbo et al. 2003; Scanlon et al. 2003; Singhal and Gupta 2007; Surinaidu et al. 2013). The EPCM approach, selected for the study case, is considered to be the most flexible method to represent the flow and transport on a regional scale (Schwarz and Smith 1988, Langevin 2003). This approach is particularly applicable for resource management purposes, where high-resolution results are less important than an overall assessment of the state of groundwater resources (Smith and Schwarz 1984; Schwarz and Smith, 1988; Panagopoulos 2012). If the EPCM is used, the discretisation should be coarse enough to be appropriate for the basic hypothesis of equivalent continuous porous medium.

The numerical code MODFLOW (McDonald and Harbaught, 1988) was used for groundwater flow, and SEAWAT (Guo and Langevin 2002) was used to simulate three-dimensional variable-density groundwater flow and transport.

The hydrogeological basin was discretised into 115,200 rectangular cells 0.48 km^2 in size (800×600 m). The cell size was considered optimal based on the large model domain, the spatial variability and data availability of hydrogeological parameters, and the flexibility and stability of the selected codes according to the EPCM hypothesis.

A no-flow boundary condition was applied along the groundwater divide of the Salento HS (northeastern border), whereas a Dirichlet boundary condition (constant head) was used along the coast. No-flow cells were defined outside the boundary; all remaining cells were active. Recharge was applied to all active cells in the top layer; the Cauchy condition was used in each cell with discharging wells.

A DEM defined the ground surface (maximum altitude 210 m asl), and 16 layers were used for the vertical discretisation. The top layer had variable thickness, but all other layers above -80 m asl were assigned a thickness of 15 m; below this altitude, the thickness was increased to 50 m until reaching the minimum altitude of -350 m asl.

The bathymetry and coastline slopes were modelled as vertical surfaces up to the model bottom (from 0 to -350 m asl), simplifying the geometry and highly reducing the run time of each calculation. In this way, the effects of the real path of groundwater outflowing through the sea bottom and through low-permeability deposits, which overlie the limestone on the sea bottom in some places, are disregarded. To compensate for the effects of this simplification, the hydraulic conductivities of the active cells adjacent to the coastal boundary were reduced according to an equivalent conductance calculation that considered sea-bottom deposits and the bathymetric slope. The final peak reduction from this consideration amounted to one order of magnitude.

The necessary hydrogeological parameters, hydraulic conductivity and storage coefficients were defined for each hydrogeological complex (Table 1). The initial parameter values were statistically assessed according to a pumping test analysis (raw data from database of CNR-IRPI Hydrogeology Group, http://hydrogeology.ba.irpi.cnr.it/), professional hydrogeological reports and data from the literature (Andreson and Woessner 1992).

3.1 Past scenarios

The first simulation (P1) was performed to define the steady-state groundwater flow and 3D salinity field in an effort to simulate nearly natural steady-state conditions (no climate change, negligible anthropogenic effects). The P1 simulation used the piezometric surface of the 1930s as initial head values, had steady-state recharge, and featured no discharging wells.

The model was calibrated through the use of an automatic code (PEST) integrated with MODFLOW. Eleven piezometric wells for which data from the 1930s were available were used for calibration (Table 2). The statistics of the validation analysis (Zheng and Bennett 2002) were as follows: mean residual error -0.12, mean absolute residual error 0.45, normalised root mean squared of residual errors 11.89%, correlation coefficient 0.903 (linear regression between observed and calculated values), and standard deviation 0.3. An analysis of model sensitivity to hydraulic conductivity variations was performed. For this purpose, the statistics were analysed for 9 cases in which the hydraulic conductivity was calculated by multiplying calibrated values by a factor ranging from 0.2 to 5. The analysis confirmed the calibrated results. Given these satisfactory results, the final steady-state piezometric surface using the calibrated hydraulic conductivity (Table 1) was plotted for each layer. The most significant layer (-50 to -65 m asl) for the effects of seawater intrusion is shown (Fig. 6).

MODPATH code (Pollock 1994) was used to plot steady-state transport path flow lines and travel times. The flow lines were used to check the quality of the piezometric results, highlighting the main recharged zones, which are located in the inner and central zones of the hydrogeological basin. The travel times defined the maximum velocity, approximately equal to 4×10^{-6} m/s, and the travel time out of the recharge zones, which was greater than 1200 years.

The output of the steady-state flow model was used as input for the density-dependent model using the SEAWAT code. A constant-concentration boundary condition was used for coastal cells. The constant concentration (salinity) was assumed equal to 38,000 and 39,500 mg/L along the Adriatic Sea and Ionian Sea, respectively (Janekovic et al. 2006; Grauel and Nernasconi 2010). The 3D spatial distribution of groundwater salinity was calculated (Fig. 7). The groundwater salinity field was consistent with existing knowledge of the spatial variability of salinity from well logs and well discharge measurements (Polemio and Limoni 2001, Polemio et al 2008).

The results of P1 were used to define a reference state against which to assess variations in other scenarios. The P1 results were considered reliable and were significant for the period 1930-79, as previously explained.

The P1 results were used as initial values for the P2 scenario using mean recharge rates calculated for 1980-1989. Similarly, the P2 final results were used as the initial values for the P3 scenario.

The assessment of well discharge was implemented from The P2 scenario.

Irrigation is of prime importance in countries dominated by the Mediterranean climate. A total of 85.6% of the irrigated surface in Italy uses groundwater resources. In the case of Murgia and Salento, 61% of the irrigation water comes from private wells, whereas 27% comes from springs and wells managed by public irrigation and reclamation consortia; the total is roughly 100% for the selected hydrogeological basin (ISTAT 2001 and 2011).

The irrigated area of the selected basin study areas, approximately 43,040 ha in the year 2000, was studied by INEA using multi-temporal infrared satellite data divulgated with reference to two portions of the study area. These portions were defined according to the reclamation consortia (INEA 2001). ISTAT (2001) collected irrigation data from 1971 via a periodic census from each land owner, divulgating them with more types of information than INEA for each of 87 municipalities within the study area; in this case, the total irrigated surface, 15,638 ha, was largely underestimated because the number of abusive private wells was very high. Because the data source with the highest spatial accuracy and the most detailed information underestimated the total irrigated surface for each type of crop, the INEA and ISTAT data were combined with rescaling information from ISTAT with emphasis on the INEA data. Five groups of crops were distinguished: herbaceous open-field crops (cereals, corn and stover), horticultural crops (including potatoes and legumes), grapes, other fruits, and olives. The specific irrigation demand of each crop group was defined on the basis of a detailed regional assessment (Apulia Region 2005), which considered soil characteristics and spatial climate variability. For each municipality, the weighted average of the specific irrigation demand, W, the weight of which was the irrigated surface area of each group of crops, was calculated. The municipal irrigation groundwater discharge was obtained by multiplying W by the municipal irrigated surface. The total annual irrigation demand was 51.77×10^6 m^3 in

2000. The irrigation groundwater discharge was considered equal to the irrigation demand. A linear function of the irrigated surface area over time was calculated with ISTAT data and applied to calculate the annual irrigation groundwater discharge for scenarios P2 and P3.

The mean annual amount of groundwater used for manufacturing or industrial purposes was approximately 0.30×10^6 m^3 in 2000. The Apulian Aqueduct (AQP), a public water company, discharged drinking water from as many as 72 wells that are concentrated in a few inland areas; the 2000 discharged volume was equal to 98.14×10^6 m^3 (Apulian Region, 2009). It was reasonable to consider the manufacturing and drinking discharge over P2 and P3 to be steady.

In each transient scenario, the annual discharge volume due to irrigation and manufacturing was converted, cell by cell, to an equivalent water height over the entire study area; this height was subtracted from the recharge, simplifying the simulation of these types of discharge. Drinking water discharge was simulated by using the coordinates of all 72 wells.

The results of the P2 and P3 models were positively validated with measured piezometric and salinity data from at least 10 wells (Fig. 1). The validation was less accurate in the case of salinity, as expected; a summary of the salinity validation in the final year of the P1 scenario is shown in Table 3.

At the end of the past scenarios (1999), a drawdown ranging from 0.1 to 1.0 m from natural or P1 conditions was observed. This piezometric decrease is consistent with other published data based on monitoring and surveys (Janekovic et al. 2006; Polemio et al. 2009b; Apulia Region 2009).

Salinity maps for each layer and year of the past scenarios are plotted and discussed. The transition zone was widespread and was mainly located in the layer from -100 to -120 m asl, as confirmed by previous log surveys and other research (Cotecchia 1977, Tulipano and Fidelibus 1988). The most representative layer in which to observe salinity variations starting from pure fresh groundwater was the layer from -50 to -65 m asl, hereinafter called the reference layer, which was selected for figures in this paper (Fig. 7). The most relevant salinity effect at the end of P2 and P3 was the upconing effect in two areas in which two drinking well fields were active; this effect was observed in situ by Cotecchia et al. (2002). The so-called threshold contour line (TCL; Polemio et al. 2009a), 500 mg/L, was plotted for the reference layer and compared with the published TCL, plotted using salinity measurements of discharging wells (Polemio and Limoni 2001, Apulia Region 2009); the comparison was almost identical considering the nature of measured data, which are influenced by salinity over a wide altitude range (screen altitude range) and by upconing.

3.2 Future scenarios

Three transient periods, called future scenarios F1, F2, and F3, were analysed: 2001-2020, 2021-2040, and 2041-2060, respectively. The final output of the previous scenario was again used as the initial condition of the next scenario, moving from P3 to F1, from F1 to F2, and from F2 to F3.

The predictive or future scenarios for the management of selected Apulian coastal groundwater resources, as with other Mediterranean aquifers, must include scenarios for or predictions of changes in rainfall, temperature, sea level, and seawater salinity.

The scientific literature on Mediterranean climate change presents interesting results. Predictive temperature models indicate an increase in temperatures in the Mediterranean basin without relevant spatial variation (Gibelin and Déqué 2003; Goubanova and Li, 2007; Alpert, et al. 2008; Jacobeit and Hertig 2008).

Mediterranean rainfall has generally decreased since the second half of the 20th century, particularly in the eastern part of the Mediterranean basin (Goubanova and Li 2007; Alpert et al. 2008). A 10.1% decrease in annual rainfall was observed from 1921 to 2001 in the Apulia region (Polemio and Casarano 2004). Based on these measurements, the rainfall trend shows non-negligible spatial variation in the Mediterranean basin; these features originate from differences among simulated scenarios (Ragab and Prudhomme 2002; Gibelin and Déqué 2003; Giorgi et al. 2004; Goubanova and Li 2007; Giorgi and Lionello 2008).

The most reliable rainfall and temperature trends were implemented into future scenarios of the study area considering the A1B scenario of the model MGME (Giorgi and Lionello 2008). The model predicts a temperature rise during the period 2001-2100 and variations in precipitation as a percentage of the mean values measured during the period 1961-1980. More specifically, temperature variations from 0.9 to 2.4 °C and rainfall variation of -3.9%, -5.9%

and -9% (from the 1961-1980 mean) were implemented in F1, F2, and F3, respectively. These predictions are in full agreement with the results of other climate change models (Boughariou et al. 2014, Mahmoud Abu-Allaban et al. 2014); as an example, rainfall variations in Apulia from -8 to -10% (reference period of 1960-1990) and temperature increases of 2.3 to 2.7 °C were evaluated for the period 2040-2070 (Garcia-Ruiz et al. 2011).

As groundwater discharge cannot be predicted, a steady discharge level for all uses at the level of 2000 was hypothesised for each future scenario. This hypothesis is approximate and will likely underestimate the future well discharge if adaptation measures are not implemented.

The seawater salinity trend was found to be approximately 0.005 g/L per year (Tsimplis et al. 2008; Adani et al. 2011). This trend was implemented in the future scenarios.

Predictions of sea level rise in the Mediterranean Sea vary considerably (a detailed discussion is beyond the scope of this article); a reasonable and prudential (meaning approximate and a likely underestimate) rise of the Ionian and South Adriatic Seas of 0.05 m was hypothesised and incorporated into scenario F3 (Tsimplis et al. 2008).

Based on these future changes, transient piezometric and salinity maps were plotted to 2060 for all layers (Fig. 6 and 7). The results show a dramatic piezometric decrease during the years up to 2060 of more than 2.5 m compared to steady-state or natural conditions (Fig. 8). These results are comparable to findings in other Mediterranean areas (Lambrakis and Kallergis 2001; Trabelsi and Zairi 2010; Boughariou et al. 2014).

Simulated salinity in 2060 shows a huge increase from steady-state conditions, greater than 5,000 mg/L in wide areas (Fig. 7 and 8). This increase is primarily located along the coastal zone, particularly in the western Ionian area. The increase and the consequent dramatic effects on drinking water resources are due to the enlargement and worsening of the upconing phenomenon that is observed around the areas of drinking groundwater discharge.

Scenarios F1 to F3 were repeated without variations in sea level and seawater salinity. Differences in the new scenarios with respect to the previous scenarios were detected up to approximately 1 km from the coast.

4. **Conclusions**

The wide, deep, coastal, and karstic aquifers that this study focuses on represent one of the most complex hydrogeological study cases. This work shows that the EPCM approach enabled a reliable hydrogeological conceptualisation and modelling that was able to simulate piezometric and salinity variations over past decades and predict future effects with a complex set of conditions. This tool should be considered reliable for testing complete and reliable management groundwater resources criteria.

The geometrical features of the coast and sea bottom, combined with hydrogeological peculiarities of sea-bottom sediments, were considered with some simplifications based on the calculation of an equivalent conductance of coastal active cells of the model.

Because of the unavailability of well discharge data for irrigation discharge, which is the main source of widespread discharge, a practical solution to defining realistic spatial assessments over time was defined.

The hypotheses at the base of predictive scenarios were defined conservatively and were finalised to assess future effects. The hypotheses were approximate and biased towards underestimation to simulate the absence of relevant adaptive management. The effective prediction of future variations in sea level and sea salinity shows that these sea variations will affect the coastal groundwater over a short period of time (up to 2060).

An evident piezometric drop was confirmed in the past for the studied aquifer; this drop will intensify in the future. The model shows the dramatic effects of drawing high levels of discharge over a narrow area in this karstic coastal aquifer, even if this area is located relatively far from the coast. The lateral intrusion and upconing effects of seawater intrusion were non-negligible in the past and will grow in the future.

The study case as a whole calls for a full management approach that defines adaptive strategies for meeting water demands, including the modification of water use technologies, water recycling, artificial recharge, and agriculture irrigation practices, to be validated with this type of numerical modelling.

References

Abbo H, Shavit U, Markel D, Rimmel A (2003) A numerical study on the influence of fractured regions on lake/groundwater interaction; the Lake Kinneret (Sea of Galilee) case. Journal of Hydrology 283, 225-243 doi:10.1016/S0022-1694(03)00273-7

Adani M, Dobricic S, Pinardi N (2011) Quality Assessment of a 1985–2007 Mediterranean Sea reanalysis. American Meteorological Society, 569-589

Alpert P, Krichak SO, Shafir H, Haim D, Osandinsky I (2008) Climatic trends to extremes employing regional modeling and statistical interpretation over the E. Mediterranean. Global and Planetary Change 63, 163–170 doi:10.1016/j.gloplacha.2008.03.003

Andreson MP, Woessner WW (1992) Applied groundwater modelling. Academic Press, San Diego

Apulia Region (2005) ACLA 2 Project Caratterizzazione agro-ecologica della Regione Puglia in funzione della potenzialità produttiva. Regione Puglia

Apulia Region (2009) Regional Water Protection Plan (PTA) Water Protection Service, General Report Area

Baalousha HM (2011) Mapping groundwater contamination risk using GIS and groundwater modelling. A case study from the Gaza Strip, Palestine Arabian Journal of Geosciences Volume 4, Issue 3-4, Pages 483-494 doi:10.1007/s12517-010-0135-0

Barrocu G (2003) Seawater intrusion in coastal aquifers of Italy. Coastal aquifers intrusion technology: Mediterranean Countries. Ministerio De Ciencia Y Tecnologia, 2, 207-223

Bertin RI (2008) Plant phenology and distribution in relation to recent climate change. Journal of the Torrey Botanical Society 135, 126–146

Biondic B, Bakalowicz M (1975) Hydrogeological aspects of groundwater protection in karst areas. Cost action 65. Final report 3-7

Boughariou E, Bouri S, Khanfir H, Zarhloule Y (2014) Impacts of climate change on water resources in arid and semi-arid regions: Chaffar Sector, Eastern Tunisia, Desalination and Water Treatment, Volume 52, Issue 10-12, 2082-2099

Brunetti M, Buffoni L, Mangianti F, Maugeri M, Nanni T, (2004) Temperature, precipitation and extreme events during the last century in Italy. Global and Planetary Change 40, 141–149 doi:10.1016/S0921-8181(03)00104-8

Candela L, von Igel W, Elorza FJ, Aronica G (2009) Impact assessment of combined climate and management scenarios on groundwater resources and associated wetland (Majorca, Spain). Journal of Hydrology 376, 510–527 doi:10.1016/j.jhydrol.2009.07.057

Ciaranfi N, Pieri P, Ricchetti G (1988) Note alla carta geologica delle Murge e del Salento (Puglia centromeridionale). Mem. Soc. Geol. It.. 41: 449-460

Civita M (2005) Idrogeologia applicata ed ambientale, Casa Editrice Ambrosiana, Milano, Italy

Cobaner M, Yurtal R, Dogan A, Motz LH, (2012) Three dimensional simulation of seawater intrusion in coastal aquifers: A case study in the Goksu Deltaic Plain. Journal of Hydrology, 464–465

COST (2005) Cost Action 621 Groundwater management of coastal karst aquifers. European Commission, Directorate-General for Research, Report EUR 21366

Cotecchia V (1977) Studi e ricerche sulle acque sotterranee e sull'intrusione marina in Puglia (Penisola Salentina). Quaderno IRSA CNR, Roma, Italy, 20

Cotecchia V, Casarano D, Polemio M (2003) Piovosità e siccità in Italia meridionale tra il 1821 ed il 2001. L'Acqua , 2, 99-106

Cotecchia V, Grassi D, Polemio M (2005) Carbonate aquifers in Apulia and seawater intrusion. Giornale di Geologia Applicata 1, 219 –231

Cotecchia V, Tulipano L (1989) Le emergenze a mare, individuate anche con tecniche di telerilevamento, come vettori di carichi inquinanti dagli acquiferi carbonatici e carsici pugliesi all'ambiente costiero II workshop Progetto Strategico, Taormina, 11-12 Dicembre 1989

Cotecchia, V, Daurù, M, Limoni, PP, Mitolo, D, Polemio, M (2002) La valutazione della vulnerabilità integrata degli acquiferi. La sperimentazione nell'area campione di Corigliano in Salento: Acque Sotterranee, v. 77, p. 9-20

Custodio E (2010) Coastal aquifers of Europe: an overview. Hydrogeology Journal 18, 269-280 doi: 10.1007/s10040-009-0496-1

Davraz A, Karaguzel R, Soyaslan I, Sener E, Seyman F, Sener S, (2009) Hydrogeology of karst aquifer systems in SW Turkey and an assessment of water quality and contamination problems. Environmental Geology 58, 973–988 doi: 10.1007/s00254-008-1577-5

Dufrense DP, Drake CW (1999) Regional groundwater flow model costruction and wellfield site selection in a karst area, Lake City, Florida. Engineer Geology 52, 129-139 doi:10.1016/S0013-7952(98)00066-0

EEA (1999) Groundwater quality and quantity in Europe. 3rd report Groundwater quality and quantity in Europe http://www.eea.europa.eu/data-and-maps/figures/groundwater-overexploitation-and-saltwater-intrusion-in-europe

El Ayni F, Manoli E, Cherif S, Jrad A, Assimacopoulos D, Trabelsi-Ayadi M (2013) Deterioration of a Tunisian coastal aquifer due to agricultural activities and possible approaches for better water management. Water and Environment Journal 27, 348–361 doi: 10.1111/j.1747-6593.2012.00354.x

El-Bihery MA (2009) Groundwater flow modeling of Quaternary aquifer Ras Sudr, Egypt. Environ.Geol. 58, 1095–1105

Ersoy AF, Gultekin F (2008) Modeling groundwater flow in the agricultural area of Gumushacıkoy (Amasya, Turkey). Bull. Eng. Geol. Environ. 67, 529–535 doi: 10.1007/s10064-008-0164-z

Garcia-Ruiz J, Lopez-Moreno JI, Vicente-Serrano SM, Lasanta-Martinez T, Begueria S (2011) Mediterranean water resources in a global change scenario. Earth Science Reviews, 105, 121-139

Giambastiani B, Antonellini M, Oude Essink GHP (2007) Saltwater intrusion in the unconfined coastal aquifer of Ravenna (Italy): A numerical model. Journal of Hydrology 340, 91– 104 doi:10.1016/j.jhydrol.2007.04.001

Gibelin AL, Déqué M (2003) Anthropogenic climate change over the Mediterranean region simulated by a global variable resolution model. Climate Dynamics 20, 327–339 doi: 10.1007/s00382-002-0277-1

Giorgi F, Bi X, Pal JS (2004) Mean interannual variability and trends in a regional climate change experiment over Europe. I. Present-day climate (1961–1990). Climate Dynamics, 22, 733–756

Giorgi F, Lionello P (2008) Climate change projections for the Mediterranean region. Global and Planetary Change, 63, 90–104 doi:10.1016/j.gloplacha.2007.09.005

Gomez JDG, Geta JAG, Scheider EG (2003) The state of seawater intrusion in Spain. Coastal aquifers intrusion technology: Mediterranean Countries. Ministerio De Ciencia Y Tecnologia, 2, 79-111

Goubanova, K, Li L (2007) Extremes in temperature and precipitation around the Mediterranean basin in an ensemble of future climate scenario simulations. Global and Planetary Change, 57, 27–42 doi:10.1016/j.gloplacha.2006.11.012

Grauel AL, Nernasconi SM (2010) Core-top calibration of δ18 O and δ 13 C of G. ruber (white) and U. mediterranea along the southern Adriatic coast of Italy. Marine Micropaleontology, 77, 175-186

Guo W, Langevin CD (2002) User's Guide to SEAWAT: A Computer Program for Simulation of Three-Dimensional Variable-Density Ground-Water Flow, U.S. Geological Survey Open-File Report 01-4340

Huntoon, PW (1994) Is it appropriate to apply porous media groundwater circulation models to karst aquifers? In: El-Kadi, A.I., (Ed.), Groundwater Models for Resources Analysis and Management, 1994 Pacific Northwest/Oceania Conference, Honolulu, HI, pp. 339–358

INEA (2001) Status of irrigation in Apulia, National Institute of Agricultural Economics Rome, Italy

IPCC (2007) Summary for Policymakers Climate Change 2007: The Physical Science Basis. Contribution of Working Group I to the Fourth Assessment Report of the Intergovernmental Panel on Climate Change

ISTAT (2001) Annual report. National Institute of Statistics, Rome, Italy, in Italian

ISTAT (2011) Annual report. National Institute of Statistics, Rome, Italy, in Italian

Jacobeit J, Hertig E (2008) Downscaling future climate change: temperature scenarios for the Mediterranean area. Global and Planetary Change, 63, 127–131 doi:10.1016/j.gloplacha.2007.09.003

Janekovic I, Antonic O, Krizan J, Bukovec D, Bakran-Petricioli T (2006) Modelling basic physical parameters in the Adriatic Sea as the basis for marine benthic habitats mapping. Ecological Modelling, 194, 6-69 doi:10.1016/j.ecolmodel.2005.10.007

Langevin, CD (2003) Simulation of Submarine Ground Water Discharge to a Marine Estuary: Biscayne Bay, Florida. Ground Water 41, 6, 758–771

Maggiore M, Pagliarulo P (2004) Circolazione idrica ed equilibri idrogeologici negli acquiferi della Puglia, geologi e territorio Periodico dell'Ordine dei Geologi della Puglia - Supplemento al n. 1/2004

Mahmoud A, El-Naqa A, Mohammed J, Hammouri N (2014) Water scarcity impact of climate change in semi-arid regions: a case study in Mujib basin, JordanArabian Journal of Geosciences 2014, 1-9

Masciopinto C (2006) Simulation of coastal groundwater remediation: the case of Nardò fractured aquifers in Southern Italy. Environmental Modelling & Software, 21, 85-97 doi:10.1016/j.envsoft.2004.09.028

McDonald MG, Harbaugh AW (1988) A modular three-dimensional finite-difference ground-water flow model. Techniques of Water-Resources Investigations of the United States Geological Survey 6

Mutasem EF, Grace R, Alameddine I Majdi AN (2014) Saltwater Intrusion in karst aquifers along the Eastern Mediterranean, 23rd SWIM, 16-20 June, Husum, Germany

Oude Essink GHP (2001) Improving fresh groundwater supply, problems and solutions. Ocean Coastal Management, 44, 429–449 doi:10.1016/S0964-5691(01)00057-6

Panagopoulos G (2012) Application of modflow for simulating groundwater flow in the Trifilia karst aquifer, Greece, 2012, Environmental Earth Science doi:10.1007/s12665-012-1630-2

Pisinaras V, Petalas C, Tsihrintzia VA, Zagana E (2007) A groundwater flow model for water resources management in the Ismarida plain, North Greece. Environmental Modeling and Assessment, 12, 75-89 doi:10.1007/s10666-006-9040-z

Polemio M, Di Cagno M, Virga R (2000) Le acque sotterranee del Gargano: risorse idriche integrative e di emergenza: Acque Sotterranee, v. 68, p. 41-58.

Polemio, M, Limoni, PP (2001) L'evoluzione dell'inquinamento salino delle acque sotterranee della Murgia e del Salento: Memorie della Società Geologica Italiana, v. 56, p. 327-331.

Polemio, M, Casarano D (2004) Rainfall and drought in southern Italy (1821-2001), in Rodda, J.C., and Ubertini, L., IAHS eds., The Basis of Civilization - Water Science?, 286, 217-227, Rome, Italy

Polemio, M. (2005) Seawater intrusion and groundwater quality in the Southern Italy region of Apulia: a multi-methodological approach to the protection. Technical Documents in Hydrology 77, UNESCO, IHP, Paris

Polemio M, Dragone V, Limoni PP (2008) Salt contamination of Apulian aquifers: spatial and time trend, 19th SWIM & 3rd SWICA jointed meeting: Cagliari, p. 115-121.

Polemio M, Dragone V, Limoni PP (2009a) Monitoring and methods to analyse the groundwater quality degradation risk in coastal karst aquifers (Apulia, Southern Italy). Environmental Earth Sciences (formerly Environmental Geology) 58, 299-312. doi:10.1007/s00254-008-1582-8

Polemio M, Dragone V, Limoni PP (2009b) The piezometric stress in the coastal aquifers of a karst region, Apulia, Italy, in Taniguchi, M., Dausman, A., Howard, K., Polemio, M., and Lakshmanan, E., eds., Sustainability of groundwater in highly stressed aquifers, Volume 329: IAHS Publications, IAHS,138-144

Polemio, M, Casarano D, Limoni PP (2010) Apulian coastal aquifers and management criteria. 21 SWIM meeting, 16-20 May, Azores ,Portugal, 203-206

Polemio M, Dragone V, Limoni PP (2011) La disponibilità di acque sotterranee in Puglia negli ultimi 80 anni, in Polemio, M., ed., Le modificazioni climatiche e i rischi naturali: Bari, CNR IRPI, p. 201-204.

Pollock DW (1989) Documentation of computer programs to compute and display pathlines using results from the U.S. Geological Survey modular three-dimensional finite-difference ground-water flow model, Open File Report 89-381.

Qahman K, Larabi A (2006) Evaluation and numerical modeling of seawater intrusion in the Gaza aquifer (Palestine). Hydrogeology Journal, 14, 713–728 doi: 10.1007/s10040-005-003-2

Ragab R, Prudhomme C (2002) Climate change and water resources management in arid and semi-arid regions: Prospective and challenges for the 21st century. Biosystems Engineering, 81, 3 doi:10.1006/bioe.2001.0013

Ranjan SP, Kazama S, Sawamoto M (2006) Effects of climate and land use changes on groundwater resources in coastal aquifers. Journal of Environmental Management, 80, 25–35 doi:10.1016/j.jenvman.2005.08.008

Rejani R, Jha MK, Panda SN (2008) Mull Simulation Modeling for Efficient Groundwater Management in Balasore Coastal basin, India. Water Resour. Manage., 22, 23-50

Scanlon ER, Mace RE, Barrett ME, Smith B (2003) Can we simulate regional groundwater flow in karst system using equivalent porous media? Case study Barton Springs Edwards aquifer, USA. Journal of Hydrology, 276, 137-158 doi:10.1016/S0022-1694(03)00064-7

Schwarz FW, Smith L (1988) A continuum approach for modelling mass transport in fractured media. Water Resource Res, 24, 8, 1360-1372.

Shammas MI, Thunvik R (2009) Predictive Simulation of Flow and Solute Transport for Managing the Salalah Coastal Aquifer, Oman. Water Resour. Manage., 23, 2941–2963 doi: 10.1007/s11269-009-9417-2

Singhal BBS, Gupta RP (2012) Applied Hydrogeology of Fractured Rocks, Kluwer Academic Publishers

Smith L, Schwarz FW (1984) An analysis of the influence of fracture geometry on mass transport in fractured media. Water Resource Res., 20, 9, 1241-125

Surinaidu L, Gurunadha S, Rames G (2013) Assessment of groundwater inflows into Kuteshwar limestone mines through flow modelling study, Madhya Pradesh, India, Arab J. Geoscience, 6: 1153-1161 doi: 10.1007/s12517-011-0421-5

Sutanudjaja EH, van Beek LPH, de Jong SM, van Geer FC, Bierkens MFP (2001) Large-scale groundwater modeling using global datasets: a test case for the Rhine-Meuse basin. Hydrol. Earth Syst. Sci., 15, 2913–2935

Trabelsi R, Zairi M (2013) Seawater intrusion characterization in the coastal section of Sfax superficial aquifer (Tunisia) 23rd SWIM, 16-20 June, Husum, Germany

Tsimplis MN, Marcos M, Somot S (2008) 21st century Mediterranean sea level rise: Steric and atmospheric pressure contributions from a regional model. Global and Planetary Change, 63, 105–111 doi:10.1016/j.gloplacha.2007.09.006

Tulipano L, Fidelibus MD (1988) Temperature of groundwaters in coastal aquifers: some aspects concerning saltwater intrusion. 10 SWIM meeting, 16-20 May, Gent, Belgium, 308-316

USA NRC National Research Council (1996) Rock Fractures and Fluid Flow- Contemporary Understanding and Applications. National Academic Press, Washington, DC, p. 551

Zheng C, Bennett GB (2002) Applied contaminant transport modeling, Jhon Wiley inc. Publication, USA

Conflicts of Interest

The authors declare no conflict of interest.

Table 1 Hydrogeological complex parameters: Kx, Ky, and Kz are the principal components of hydraulic conductivity after calibration (m/s); Sy is specific yield; Ss is specific storage (1/m); and n_e is effective porosity.

Complex	Kx	Ky	Kz	Sy	Ss (1/m)
Limestones	$9\ 10^{-4}$	$9\ 10^{-4}$	10^{-4}	0.2	10^{-6}
Calcarenites and calcilutites	$1\ 10^{-5}$	$1\ 10^{-5}$	$5\ 10^{-6}$	0.2	10^{-5}
Calcarenites	$5\ 10^{-5}$	$5\ 10^{-5}$	$5\ 10^{-6}$	0.3	10^{-5}
Clays	10^{-8}	10^{-8}	10^{-9}	0.1	10^{-3}
Sands	$9\ 10^{-5}$	$9\ 10^{-5}$	$9\ 10^{-6}$	0.2	10^{-4}

Table 2 Piezometric steady-state calibration data. The observed head was calculated as the mean value of all available measurements from the 1930s.

Well	Well bottom (m asl)	Observed head (m asl)	Calculated head (m asl)	Residual (m)
1	-72	2.23	3.15	-0.92
2	-54	3.43	4.02	-0.59
3	-90	3.52	4.29	-0.77
4	-51	3.67	3.99	-0.32
5	-55	4.31	4.79	-0.48
6	-26	4.56	4.70	-0.14
7	-52	4.63	4.34	0.29
8	-73	5.06	4.96	0.10
9	-40	5.22	4.70	0.52
10	-61	5.32	5.17	0.15
11	-158	5.86	5.09	0.77

Table 3 Transient salinity validation of scenario P1 (1980-1989, 1989 data) (mg/L). The observed head was calculated as the mean value of all available measurements from each year.

Well	Observated Concentration	Calculated Concentration	Residual
12	320	300	20
13	300	890	-590
14	410	530	-120
15	440	360	80
16	1150	1240	-90
17	320	510	-190
18	340	500	-160
19	380	280	10
20	440	620	-180
21	880	814	66

Reference to be cited:
Romanazzi, A., Gentile, F., Polemio, M.: Modelling and management of a Mediterranean karstic coastal aquifer under the effects of seawater intrusion and climate change, Environmental Earth Sciences, 74 (1), 115-128, DOI: 10.1007/s12665-015-4423-6, 2015.

FIGURES

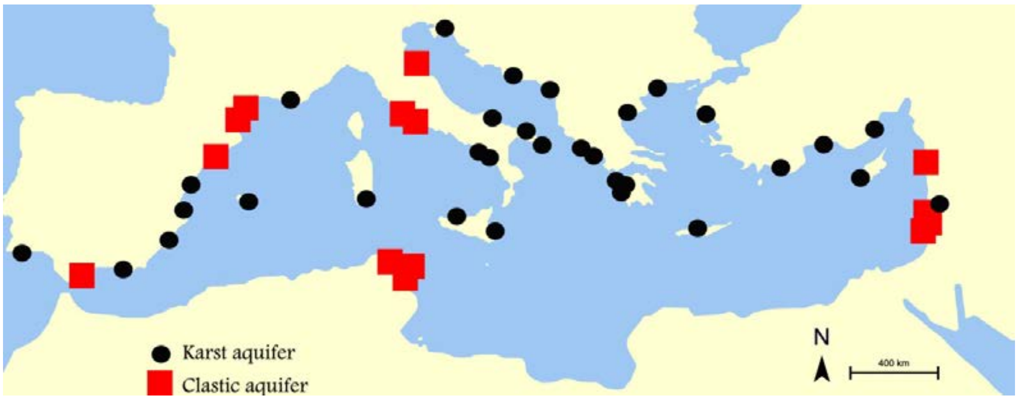

Figure 1 Mediterranean coastal aquifers highly affected by groundwater quality degradation due to seawater intrusion.

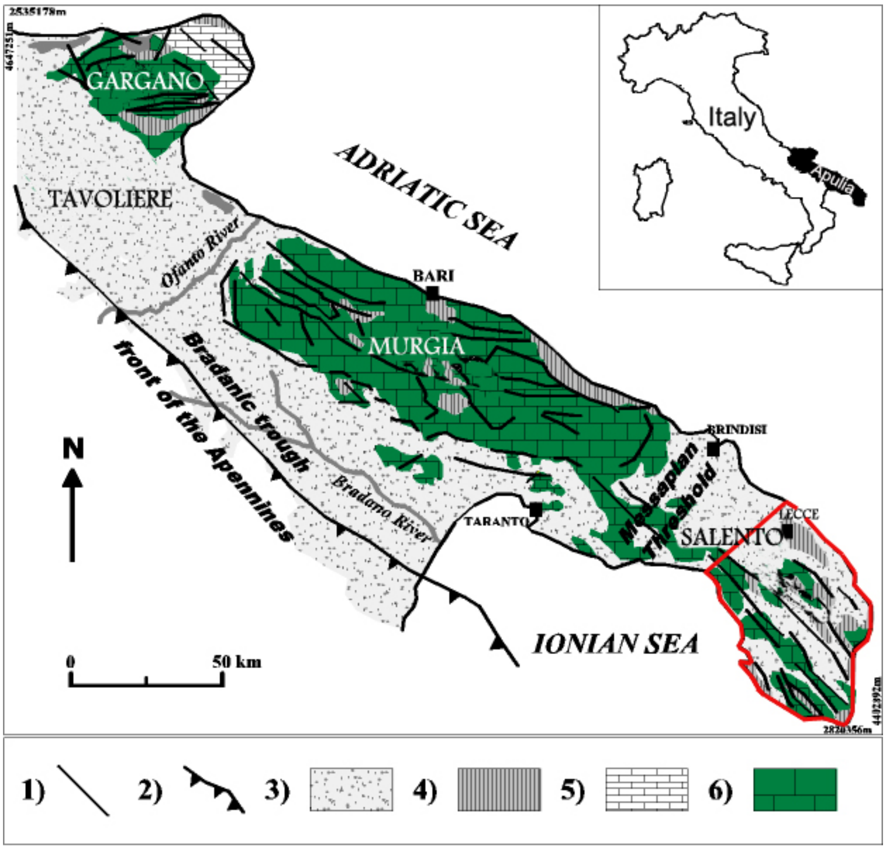

Figure 2 Schematic geologic map of Apulia. (1) Fault, (2) front of the Apennines, (3) recent clastic cover (Pliocene–Pleistocene), (4) bioclastic carbonate rocks (Palaeogene) and calcarenites (Miocene), (5) chert-carbonate rocks (Upper Jurassic-Cretaceous), and (6) carbonate platform rocks (Upper Jurassic-Cretaceous). The red line shows the boundary of the selected hydrogeological basin.

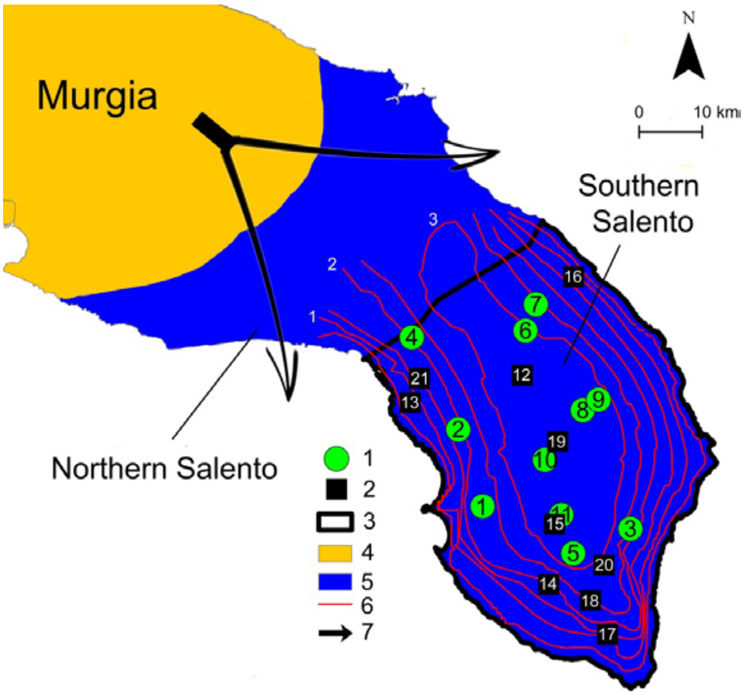

Figure 3 Selected hydrogeological basin (SHB) and piezometric surface map of the 1930s (PSM30). 1) piezometric steady-state calibration, 2) validation well, 3) SHB, 4) Murgia hydrogeological structure, 5) Salento hydrogeological structure, and 6) PSM30 (m asl).

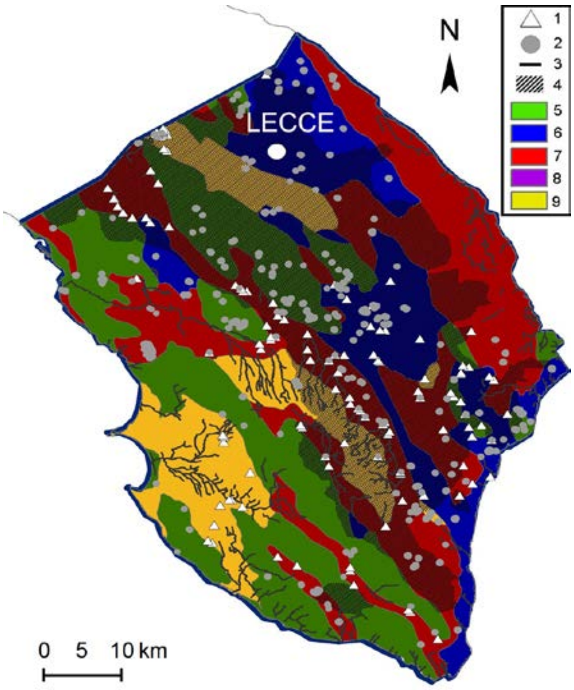

Figure 4 Karstic surface features and hydrogeological complexes. 1) Sinkhole, 2) doline, 3) karstic drainage network, 4) endorheic area, 5) limestone, 6) calcarenite-calcilutite, 7) calcarenite, 8) clay (does not outcrop), and 9) sand-conglomerate-calcarenite.

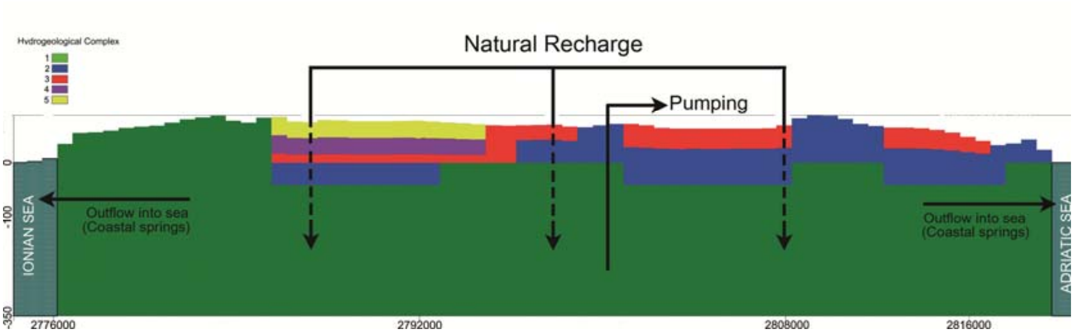

Figure 5 Schematic west-east section of the hydrogeological conceptual model. Hydrogeological complex: 1) limestone, 2) calcarenite-calcilutite, 3) calcarenite, 4) clay, and 5) sand-conglomerate-calcarenite.

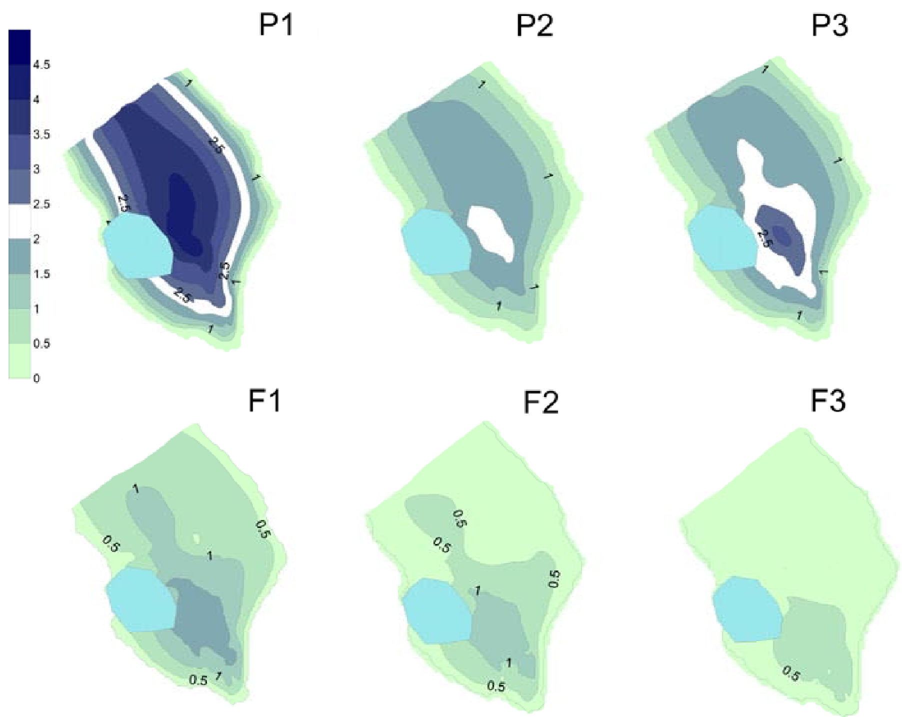

Figure 6 Piezometric maps of past (P1-P3) and future or predictive (F1-F3) scenarios at the reference layer (from -50 to -65 m asl): (P1) Steady-state simulation; results of the last year of each transient period (P2) 1989; (P3) 1999; (F1) 2020; (F2) 2040; and (F3) 2060. The light blue area denotes the shallow aquifer.

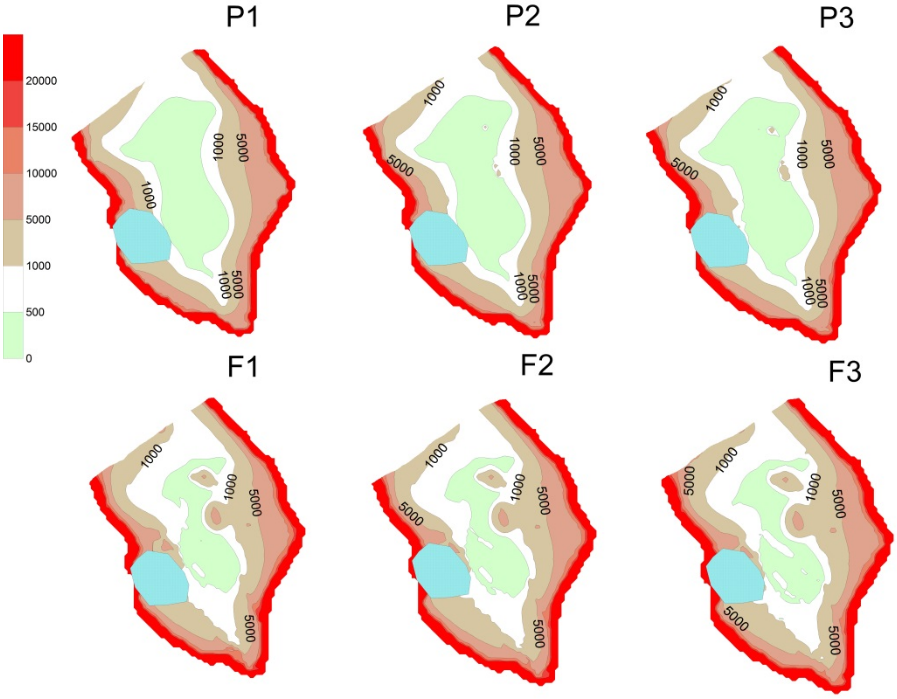

Figure 7 Salinity maps of past (P1-P3) and future or predictive (F1-F3) scenarios at the reference layer (from -50 to -65 m asl): (P1) Steady-state simulation; results of the last year of transient simulation of each period (P2) 1989; (P3) 1999; (F1) 2020; (F2) 2040; and (F3) 2060. The light blue area denotes the shallow aquifer.

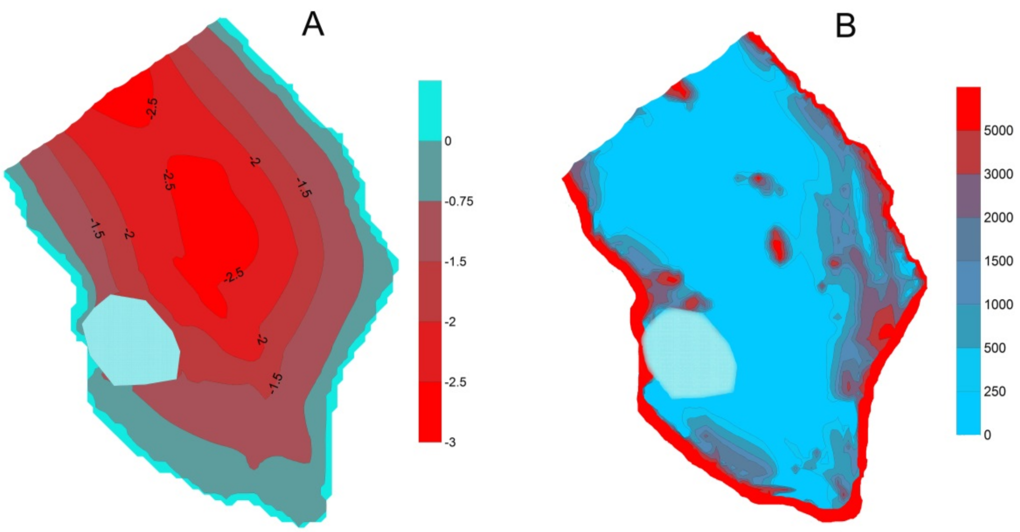

Figure 8 Piezometric (A, m) and salinity (B, mg/L) variation map for the reference layer (layer -50 to -65 m asl) in the year 2060, in reference to natural or steady state conditions. The light blue area denotes the shallow aquifer.